Cobalt Loading Effects on the Structure and Activity for Fischer-Tropsch and Water-Gas Shift Reactions of Co/Al_2O_3 Catalysts

Tavasoli, Ahmad*+; Sadaghiani, Kambiz; Nakhaeipour, Ali; Ahangari, Masoumeh
Research Institute of Petroleum Industry, P. O. Box 18745-4163 Tehran, I.R. IRAN

ABSTRACT: *An extensive study of Fischer-Tropsch synthesis (FTS) on alumina-supported cobalt catalysts with different amounts of cobalt is reported. Up to 40 wt % of cobalt, is added to the catalysts by impregnation method. The effect of the cobalt loading on the reducibility of the cobalt oxide species, dispersion of the cobalt, average clusters size, water-gas shift (WGS) activity and activity and selectivity of FTS is investigated. Increasing the cobalt loading resulted in increasing the average cobalt cluster size, improvements in the reducibility of Co_3O_4, decreasing the cobalt surface interaction with the support and decreasing the dispersion of cobalt. The maximum concentration of active surface Co^o sites and FTS activity are achieved for the 34 wt% cobalt loading. While the maximum WGS activity is achieved for the 40 wt % cobalt loading. The methane selectivity in the catalyst with 40 wt % of cobalt loading was about 43.7 % less compared to that of the less reducible 8 wt % cobalt catalyst. The C_5^+ selectivity for the 40 wt % cobalt catalyst was 60.8% higher than that of the 8 wt % Cobalt catalyst.*

KEY WORDS: *Cobalt catalyst, Fischer-Tropsch, Water-gas shift, Activity, Selectivity.*

INTRODUCTION

The increasing demand for high-quality and environmentally friendly transportation fuels together with the technological improvements achieved in the recent years in gas-to-liquid (GTL) processes making them more efficient and cost competitive has renewed the interest of using natural gas as a potential source of hydrocarbons [1]. The FTS process has shown to be catalyzed by certain transition metals, with Co, Fe, and Ru presenting the highest activity [2,3]. Among them, cobalt catalysts are the preferred catalysts for FTS based on natural gas because of their high activity for FTS, high selectivity to linear hydrocarbons, low activity for the water gas shift (WGS) reaction, more stability toward deactivation by water (a by-product of the FTS reaction), and low cost compared to Ru. In order to achieve high surface active sites (Co^o), cobalt precursors are dispersed on porous carriers, with SiO_2, Al_2O_3, and to a lesser extent TiO_2 being the most frequently used. Due to its high resistance to attrition and its ability to stabilize a small cluster size, Al_2O_3 is a particularly appealing

* *To whom correspondence should be addressed.*
+ *E-mail: tavassolia@ripi.ir*
1021-9986/07/1/9 8/$/2.80

support for cobalt based FTS catalysts [4]. One important focus in the development of these catalysts is the improvement of the catalyst activity by increasing the number of active metal sites that are stable under reaction conditions. However, due to the strong interactions of cobalt species with the support more insight is needed into understanding the effect of the loading and size distribution on both the physico-chemical properties and performance of these catalysts [5]. *Iglesia et al.* showed that the FT synthesis rates per total cobalt atoms increase linearly with increasing metal dispersion irrespective of the nature of the support used [6]. In other words, the turnover rates are not influenced by support identity, and thus the catalyst activity should be proportional to the number of surface cobalt metal (Co^o) sites. *Jacobes et al.* have shown that, increasing the cobalt loading, will improve the reducibility by decreasing the interactions with the support [7]. By working at atmospheric pressure and differential conditions, *Khodakov et al.* observed an increase of the turnover rates by increasing the particle size of cobalt supported on mesoporous silicas of different pore size [8]. More recently *Tavasoli et al.* by addition of different loadings of Re and Ru to 15 wt % Co/Al_2O_3 catalyst, have shown that, the final density of active Co^o sites depends on two main parameters, i.e., cobalt dispersion and the degree of reducibility of the supported oxidize cobalt species [3]. Ideally, optimum cobalt catalysts should be prepared by achieving high dispersions of highly reducible cobalt species at cobalt loadings as high as possible [1].

Due to high cost of cobalt, it is important to determine the appropriate loading of cobalt to maximize the availability of active cobalt surface sites for participation in the reaction, after catalyst activation. In this work a series of Co/Al_2O_3 catalysts were prepared with different loadings of cobalt (8-40 wt %) by impregnation method. The effect of the cobalt loading on the reducibility of the cobalt oxide species, dispersion of the cobalt, average clusters size, activity for the WGS reaction and activity and selectivity of FTS is investigated. As it is evident from this work, the amount of loading of the cobalt plays an important role in the accessing of cobalt metal sites for FTS reaction.

EXPERIMENTAL

Catalyst preparation

All catalysts were prepared with slurry impregnation of cobalt nitrate ($Co(NO_3)_2.6H_2O$ 99.0 %, Merck) solution on alumina (Conndea Vista Catalox B γ-alumina, 200 m^2/g) as the support. The alumina was calcined at 500 ^oC for 10 h prior to its impregnation with cobalt nitrate aqueous solution. C_1 and C_2 were prepared with 2 and 3 molar aqueous solutions respectively. Other catalysts were prepared by 5 molar solutions. For the C_3, C_4, C_5, and C_6, 1, 2, 3 and 4 sequential impregnation was accomplished respectively. After each step, the catalyst was dried at 120 ^oC and calcined at 450 ^oC for 3 h with a heating rate of 1 ^oC/min. The cobalt loadings were verified by an inductively coupled plasma (ICP) AES system. The composition of the catalysts is listed in table 1.

Table 1: The composition of the catalysts.

Catalyst	C_1	C_2	C_3	C_4	C_5	C_6
Wt % Cobalt	8	11	16	24	34	40

X-ray diffraction

XRD measurements were conducted with a Philips PW1840 X-ray diffractometer with monochromatized Cu/K_α radiation. Using the Scherrer equation, the average size of the Co_3O_4 crystallites in the calcined catalysts was estimated from the line broadening of a Co_3O_4 at 2θ of 36.8^o. The Co_3O_4 particle sizes in the calcined samples were then converted to the corresponding cobalt metal diameters in reduced catalysts by considering the relative molar volumes of Co^o and Co_3O_4 using the equation [9-11]:

$$d(Co^o) = 0.75 \times d(Co_3O_4)$$

Temperature programmed reduction

Temperature programmed reduction (TPR) spectra of the catalysts were recorded using a Micromeritics TPD-TPR 290 system equipped with a thermal conductivity detector. The catalyst samples were first purged in a flow of argon at 300 ^oC, to remove traces of water, and then cooled to 40 ^oC. The TPR spectra of 50 mg of each sample were obtained using 5.1 % hydrogen in argon gas mixture with a flow rate of 40 cm^3/min. The samples were heated from 40 to 1000 ^oC with a heating rate of 10 ^oC /min.

Hydrogen chemisorption and reoxidation

The amount of chemisorbed hydrogen was measured

Table 2: Catalysts characterization data.

Catalyst Name	C_1	C_2	C_3	C_4	C_5	C_6
XRD $d_{Co_3O_4}$ (nm)	10.7	14.1	16.5	18.5	31	38
XRD d_{Co} (nm)	7.95	10.6	12.4	13.9	23.3	28.5
First TRR peak temperature (^oC)	374	370	368	368	360	322
Second TRR peak temperature (^oC)	624	608	605	600	597	571
1st Peak reducibility ratio	1	1.5	2.7	3.1	3.2	3.1
2nd Peak reducibility ratio	1	1.35	1.5	2.1	3.2	3.3
Reducibility ratio of TPR	1	1.37	1.88	2.6	3.1	3.2

using the micromeritics TPD-TPR 290 system. 0.22 g of the calcined catalysts were reduced at 400 ^oC for 12 h and then cooled to 100 ^oC under hydrogen flow. Then the flow of hydrogen was switched to argon at the same temperature, which lasted about 30 minutes in order to remove the weakly adsorbed hydrogen. Afterwards the temperature programmed desorption (TPD) of the samples was obtained by increasing the temperature of the samples, with a ramp rate of 10 ^oC/min, to 400 ^oC under the argon flow. The TPD spectrum was used to determine the cobalt dispersion and its surface average crystallite size. After the TPD of hydrogen, the sample was reoxidized at 400 ^oC by pulses of 10 % oxygen in helium to determine the extent of reduction. It is assumed that Co^o is oxidized to Co_3O_4. The calculations are summarized below. The calculated dispersion and diameter are corrected by the percentage reduction [3,5].

$$\%\,\text{Dispersion} = \frac{\text{number of Co}^o\text{ atoms on surface}}{\text{number of Co atoms in sample}} \times 100$$

$$\text{Fraction reduced} = \frac{\text{O}_2\text{ uptake} \times 2/3 \times \text{atomic weight}}{\text{Percentage metal}}$$

$$\text{Diameter} = \frac{6000}{\text{density} \times \text{maximum area} \times \text{dispersion}}$$

REACTION TESTING

The catalysts were evaluated in terms of their Fischer-Tropsch synthesis (FTS) activity (g HC produced/ g cat/ min), activity for the water gas shift (WGS) reaction (g CO_2 produced/ g cat/ min) and selectivity (the percentage of the converted CO that appears as a hydrocarbon product) in a tubular fixed-bed micro-reactor. Typically, 0.5 g of the catalyst was charged into a 1/4" stainless steel tube, as the reactor. The reactor was placed in a molten salt bath with a stirrer to ensure a uniform temperature along the catalyst bed. The temperature of the bath was controlled via a PID temperature controller. Separate Brooks 5850 mass flow controllers were used to add H_2 and CO at the desired rate to a mixing vessel that was preceded by a lead oxide-alumina containing vessel to remove carbonyls before entering to the reactor. Prior to the activity tests, the temperature was raised to 400 ^oC with a heating rate of 1 ^oC /min and the catalysts were reduced in a flow of H_2 for 12 h. The FTS tests were carried out at 220 ^oC, 1 bar, and a H_2/CO ratio of 2. The effluents of the reactor were analyzed for CO, CO_2, and C_1-C_{25} hydrocarbons, using an on-line Varian 3800 gas chromatograph. FTS rate, WGS rate and different product selectivities were calculated based on the GC analyses. Anderson-Schultz-Flory (A-S-F) distribution line was plotted for C_4-C_{25} products to determine the chain growth probability, α.

RESULTS AND DISCUSSION

XRD patterns for the calcined Co/Al_2O_3 with different loading of cobalt are shown in Fig. 1. The peaks at 46.1 and 66.5^o correspond to γ-alumina, while the other peaks, except the 49^o peak, which is attributed to the cobalt aluminate [3,5], relate to the different crystal planes of Co_3O_4. The peak of 36.8^o is the most intense peak of Co_3O_4 in all catalysts. Fig. 1 represents that the peaks become narrower, indicating an increase of the mean Co_3O_4 crystallite size, with increasing cobalt content [1]. Table 2 shows the average Co_3O_4 particle size of different catalysts and corresponding cobalt metal (Co^o) diameters in reduced catalysts calculated from XRD spectrum and Scherrer equation. This table shows that by increasing the

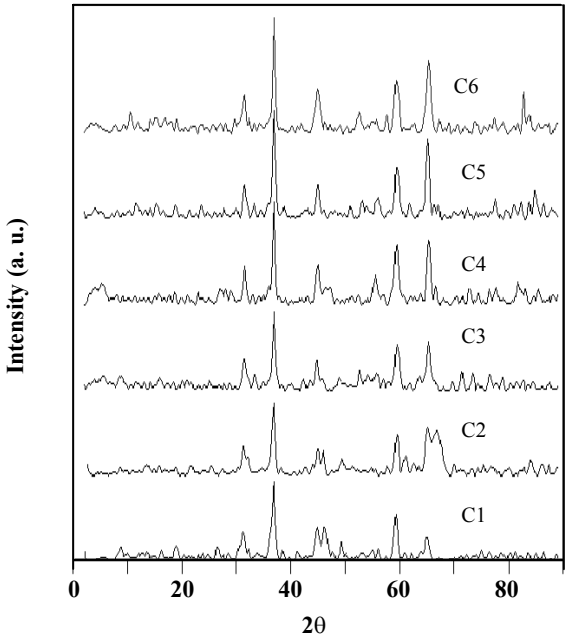

Fig. 1: XRD patterns of calcined catalysts.

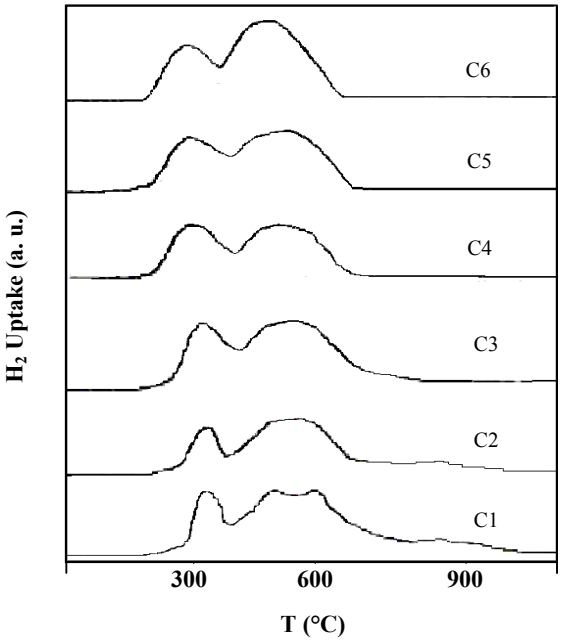

Fig. 2: TPR patterns of calcined catalysts from 40-1000 °C.

cobalt loading, Co_3O_4 particle size and corresponding Co^o diameters increases. Loading of more cobalt on the same surface causes aglomerization of particles, which in turn leads to higher cluster sizes. The cobalt aluminate peak (49^o) is better distinguishable for the C_1, C_2, and C_3 catalysts. Fig. 1 denotes that increasing the cobalt loading results in disappearance of the cobalt aluminate peak from XRD spectrum of the Co/Al_2O_3 catalyst. The disappearance of the cobalt aluminate peak in the catalysts with higher cobalt loading can be attributed to the increase in the average cluster size (table 2) and the resulting loss of interaction with the support. Part of the cobalt in the low cobalt loading catalysts strongly interacts with the support and results in the formation of cobalt aluminate.

Temperature programmed reduction is a powerful tool to study the reduction behavior of oxidation phases; in some cases it is also possible from the reduction profiles of supported oxides to obtain useful information about the degree of interaction of the active metal with the support [3,5]. The influence of cobalt loading on the reduction behavior for the different loading Co/Al_2O_3 catalysts is shown in Fig. 2 and table 2. In Fig. 2, the first peak is typically assigned to the reduction of Co_3O_4 to CoO, although a fraction of the peak likely comprise the reduction of the larger, bulk-like CoO species to Co^o.

The second broader peak, with a shoulder in some TPR spectra, is mainly assigned to the second step reduction, which is mainly reduction of CoO to Co^o. It also includes the reduction of cobalt species that interact with the support, which extends the TPR spectra to higher temperatures, such as the broad peak for C_1, C_2 and C_3 catalysts [3,5,7,12,13]. As shown in Fig. 2, increasing the cobalt loading significantly decreases the relative intensity of the second reduction peak shoulder and causes its tailing to get shorter, suggesting a higher degree of reduction. The relative contribution of the species reduced at high temperatures (500-700 ^oC) to the overall reduction pattern decreased and the maximum temperature for these species shifted to lower temperatures, indicating a lower strength of interaction, with increasing cobalt loading.

On the other hand, a significantly different reduction pattern was observed for the catalyst with 8 wt % cobalt loading and to a leaser extent 11 wt % cobalt loading catalyst (i. e. C_1 and C_2). A reduction feature for these samples was observed in the temperature range of 700-950 ^oC, with a maximum centered at about 800 ^oC. Such a high reduction temperature might be assigned to the reduction of cobalt aluminate species formed by reaction of highly dispersed CoO with the alumina. In fact, cobalt aluminates were shown to reduce at temperatures well

Table 3: H_2 temperatures programmed desorption and pulse reoxidation of catalysts.

Catalyst Name	C_1	C_2	C_3	C_4	C_5	C_6
μ mole H_2 desorbed /g cat.	42	56	75	87	71	60
μ mole O_2 Consumed /g cat.	179	290	547	1278	2410	3009
% Reduction	19.6	23	31.3	48.8	65	68.9
% Dispersion (Total Co)	6.14	5.96	5.48	4.24	2.44	1.76
% Dispersion (Reduced Co)	31.3	25.9	17.5	8.69	3.75	2.55
d_p(nm) (Total Co)	16.66	17.16	18.67	24.12	41.93	58.13
d_p(nm) (Reduced Co)	3.27	3.95	5.85	11.77	27.28	40.12

above 800 ^oC, while bulk Co_3O_4 became completely reduced at temperatures below 500 ^oC [3,5]. All these features suggest part of the cobalt in the low cobalt loading catalysts strongly interacts with the support, as also evidenced from XRD patterns.

Table 2 shows the temperatures of the TPR peak's maximum. As shown in this table, increasing the cobalt loading significantly shifts both TPR peaks to the lower temperatures, suggesting an easier reduction process. Addition of cobalt loading from 8 to 40 wt % results in a decrease in the temperature of the first TPR peak from 374 to 322 ^oC and the temperature of the second TPR peak from 624 to 571 ^oC. This indicates that by increasing the cobalt loading the amount of the species reduced at high temperatures (500-700 ^oC) decreases. These differences are attributed to the increase in the average cluster size (table 2) and the resulting loss of interaction with the support.

Table 2 also shows the reducibility ratio for the whole TPR profile and that of the 1st and 2nd peaks, defined by the ratio of the areas of the corresponding peaks to that for less reducible C_1 catalyst. This is proportional to the amount of hydrogen consumed. Moving upward from the 8 to 40 wt % cobalt loaded catalyst, results in a significant improvement in the reducibility of the catalyst (3.2 times). At cobalt loading of 24 wt % and higher, the total reducibility ratio for the whole TPR profile is almost tripled, which is attributed to the reduction of bulk-like CoO species. Bulk Co_3O_4 became completely reduced at temperatures below 500 ^oC [1,7,14].

The results of hydrogen temperature programmed desorption (TPD) and oxygen titrations of the catalyst samples are given in table 3. This table shows that the hydrogen uptake increases with increasing the amount of cobalt added up to 24 wt % then decreases. In agreement with the results of TPR, the percentage reduction shows a remarkable increase with the increasing of the amount of cobalt, while the dispersion of the cobalt crystallites, calculated based on the total amount of cobalt and the amount of reduced cobalt, decreases significantly. This table shows that increasing the amount of cobalt causes a remarkable increase in cobalt particle size, which is due to the aglomerization of the cobalt crystallites with increasing the cobalt loading. Larger cobalt clusters have lower interaction with alumina support and reduce more easily [1, 7,12,13].

Fig. 3 presents the results of % dispersion, % reduction, Fischer-Tropsch synthesis rate (g HC produced/ g cat. / min) and number of active sites for different catalysts. Number of active cobalt sites was defined as:

$$\text{No. Act. Si.} = \text{wt of Co} \times \text{Fra. Red.} \times \text{Dis.} \times N_A \times \text{MW}$$

Where N_A is Avogadro's number and MW is molecular weight of cobalt. It is also worthy to mention that no significant activity has been reported for the FT process in the absence of catalyst [1]. Basically this can be due to the short length of reactor and in the opinion of the author no significant conversion should occur relative to very noticeable conversion of synthetic gas to hydrocarbons [1].

This figure reveals that with increasing the amount of cobalt loading, dispersion decreases and the fraction ofreduced cobalt increases. FTS rate shows a remarkable increase, passes through a maximum at cobalt loading of 34 wt % and then starts to decrease. This figure reveals

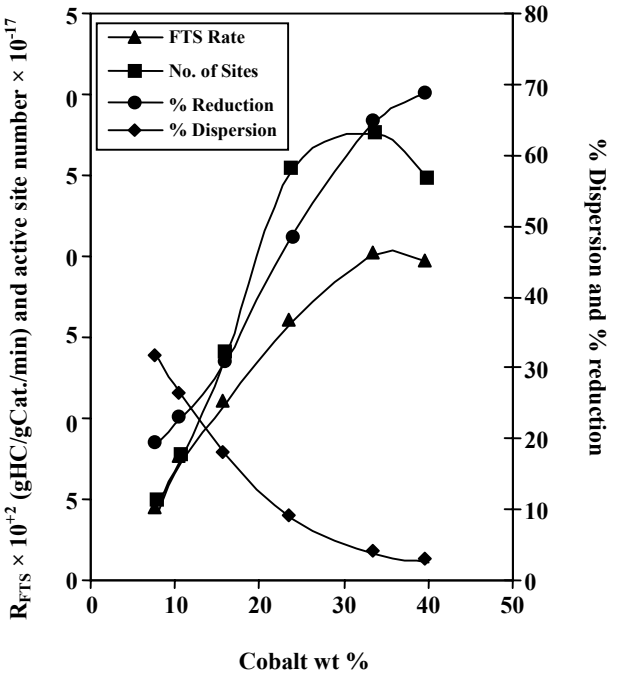

Fig. 3: Variation of % dispersion, % reduction, Fischer-Tropsch synthesis rate (g HC produced/ g cat. / min) and number of active sites with cobalt loading (T =220 °C, P=1 bar and $H_2/CO = 2$).

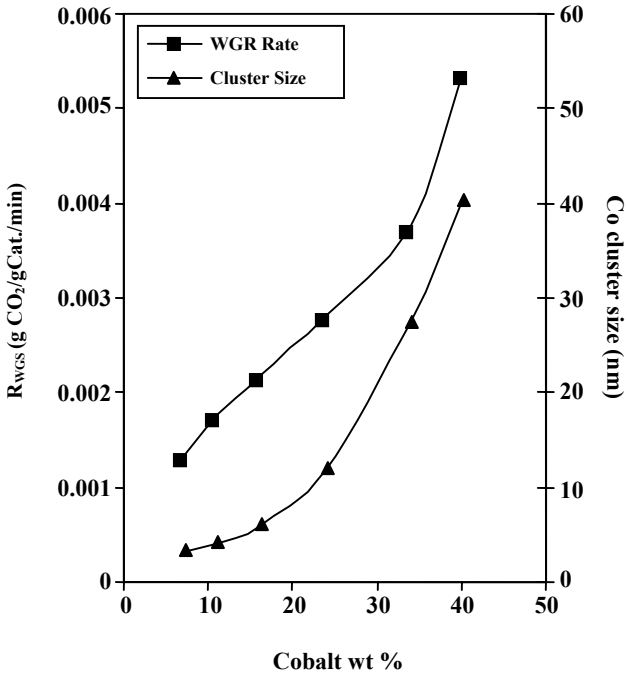

Fig. 4: Variation of cobalt cluster size and water gas shift reaction rate with cobalt loading (T = 220 °C, P = 1 bar and $H_2/CO = 2$).

that the FTS rate increases, in accordance with the reduction percentage, with addition of cobalt loading up to 34 wt %, and then starts to decrease. Meanwhile, however, the FTS rate is seen to keep on increasing, in contrast to the percentage dispersion, with addition of cobalt loading up to 34 wt %, and then decreases. This trend implies an intrinsic activity of cobalt irrespective of cobalt content, percentage reduction and dispersion. Fig. 3 reveals that the Fischer-Tropsch activity of cobalt catalysts is strongly proportional to the number of active cobalt sites. The maximum activity obtained thus reflects the inverse trends of cobalt dispersion and extent of reduction observed when increasing cobalt loading. Therefore, the maximum concentration of surface Co^o sites and FTS activity are achieved for the 34 wt % cobalt sample presenting a good dispersion and high reducibility. However, this value is a proper loading when γ–alumina with about 200 m^2/g surface area and 0.7 void fraction is the catalyst support.

The effect of the cobalt loading on cobalt cluster size and water gas shift reaction rate is shown in Fig. 4. Water gas shift reaction rate is equal to the formation rate of CO_2 (R_{FCO2}) and can be defined by [15]:

$$R_{WGS} = R_{FCO2} = \text{g } CO_2 \text{ produced / g cat. / min}$$

This figure shows that, the cobalt cluster size and water gas shift reaction rate increases by increasing the cobalt loading. This may be attributed to the tendency of larger cobalt particles for H_2O adsorption, which presumably participate in the water-gas shift reaction, and leads to the production of CO_2. Also, the increase of the CO_2 formation rate can be attributed to the increase in water partial pressure, due to an increase in FTS reaction rate [1,5].

Fig. 5 shows the effect of cobalt loading on the selectivity of Fischer-Tropsch synthesis to CH_4, C_2-C_4 light gases and C_5^+ products. It clearly shows that, the methane and C_2-C_4 light gases selectivity reduces and that of C_5^+ increases by increasing the cobalt loading.

Moving upward from the 8 to 40 wt % cobalt loaded catalyst (increasing the average cluster size form 3.27 to 40.12), results in 60.8 % improvement in the C_5^+ selectivity of the catalysts. At the same time the 40 wt % catalyst, show 43.7 % lower selectivity to methane. Also 8 wt % catalyst, show 40.6 % higher selectivity to C_2-C_4 light gaseous products. This Figure clearly demonstrates

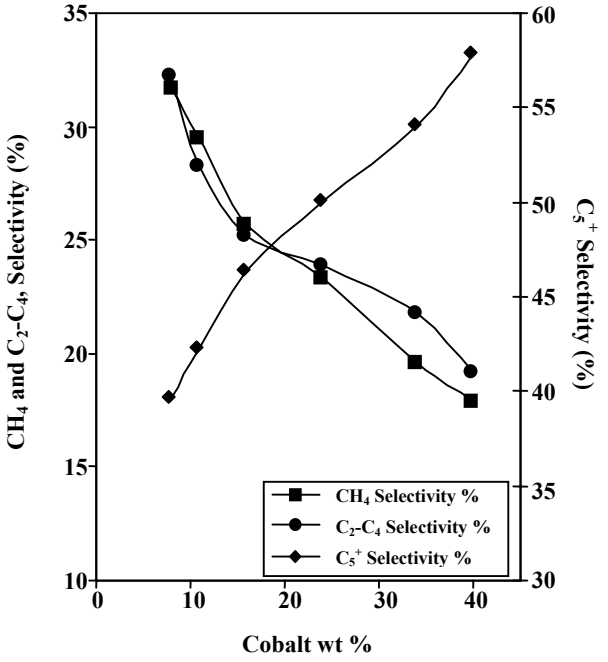

Fig. 5: Variation of CH_4, C_2-C_4 and C_5^+ selectivity of FTS with cobalt loading (T = 220 °C, P = 1 bar and H_2/CO = 2).

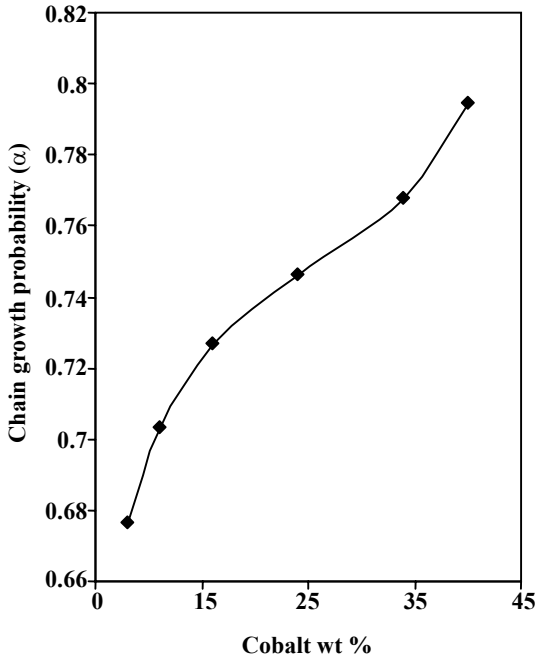

Fig. 6: Variation of Chain growth probability (α) of FTS with cobalt loading (T = 220 °C, P = 1 bar and H_2/CO = 2).

that the larger cobalt particles are more selective to higher molecular weight hydrocarbons and the smaller particles are selective for methane and light gases. It seems that the steric hindrance for dissociative adsorption of CO and -CH_2- monomer and addition of this monomer to the growing chain is less in the larger cobalt clusters. On the other hand, chain propagation and growth probability of the larger clusters is more than the smaller ones [1].

Chain growth probability (α) of FTS on different catalysts is presented in Fig. 6 product distribution shows a distinct shift to higher molecular weight hydrocarbons, which is clear from an ascending trend in chain growth probability, α, with increasing the cobalt loading of catalysts. The inclination C_5^+ hydrocarbons selectivity, reported in Fig. 5 agrees with this trend.

CONCLUSIONS

The XRD and TPR screening indicated that the interaction between cobalt surface species and the support decreased greatly by increasing the cobalt loading. Increasing the cobalt loading increased the average cobalt cluster size and improved the reducibility of the catalyst. However the percentage dispersion decreased. From a catalytic activity stand point, increasing the cobalt loading caused a remarkable increase, passed through a maximum at cobalt loading of 34 wt % and then slightly decreased.

The catalyst FTS activity is directly proportional to the amount of reduced surface cobalt metal sites. The WGS activity increased by increasing the average cluster size and cobalt loading. The methane and light gaseous hydrocarbons selectivity decreased and that of C_5^+ increased by increasing the cobalt loading of the catalysts. The larger cobalt particles are more selective to higher molecular weight hydrocarbons and CO_2 and the smaller particles are selective for methane and light gaseous hydrocarbons.

Nomenclatures

P	Pressure (bar)
T	Temperature (°C)
R	Rate (g/g cat. /min)
S	Selectivity (%)

Abbreviations

GTL	Gas-to-liquid
FTS	Fischer-Tropsch Synthesis
WGS	Water-gas shift
XRD	X-ray diffraction
TPR	Temperature programmed reduction

GC	Gas chromatograph
TPD	Temperature programmed desorption
ICP	Inductively coupled plasma

Subscripts

n	Carbon number
f	Formation
p	Particle

Received : 28th January 2006 ; Accepted : 6th July 2006

REFERENCES

[1] Tavasoli A., Ph. D. Thesis, University of Tehran, Tehran, Iran, (2005).
[2] Vannice, M.A., *J. Catal.*, **50**, p. 228 (1977).
[3] Tavasoli, A., Mortazavi, Y., Khodadadi, A., Sadagiani, K., *Iran. J. Chem. Chem. Eng.*, **24** (35), p. 9 (2005).
[4] Espinozan, R.L., Visagie, J.L., Van Rerge, P.J., Bolder, F.H., US patent 5733839 (1998).
[5] Tavasoli, A., Mortazavi, Y., Khodadadi, A., Karimi, A., *Iran. J. Chem. Chem. Eng.*, **24** (36), p. 25 (2005).
[6] Iglesia, E., Soled, S.L., Fiato, R.A., *J. Catal.*, **137,** p. 212 (1992).
[7] Jacobs, G., Das, T., Zhang, Y., Li, J., Racoillet, G., Davis, B.H., *App. Catal. A.*, **233,** p. 263 (2002).
[8] Khodakov, A. Y., Griboval, A., Bechara R., Zholobenko, V.L., *J. Catal.*, **206,** p. 230 (2002).
[9] Panpranot, J., Goodwin, J.G., Sayari, A., *Catal. Today* **77,** p. 269 (2002).
[10] Wang, Y., Noguchi, M., Takahashi, Y., Ohtsuka, Y., *Catal. Today*, **68,** p. 3 (2001).
[11] Martinez, A., Lopez, C., Marquez, F., Diaz, I., *J. Catal.*, **220,** p. 486 (2003).
[12] Jacobs, G., Patterson, P. M., Zhang, Y., Das, T., Li, J., Davis, B.H., *Appl. Catal. A*, **233,** p. 215 (2002).
[13] Jacobs, G., Das, T., Patterson, P. M., Li, J., Sanchez, L., Davis, B.H., *Appl. Catal. A*, **247**, p. 335 (2003).
[14] Hilmen, A.M., Schanke, D., Hansesen, K.F., Holmen, A., *Appl. Catal. A*, **186,** p. 63 (1999).
[15] Ngantsoue-Hoc, W., Zhang, Y., O'Brien, R.J., Luo, M., Davis, B.H., *Appl. Catal. A*, **236**, p. 77 (2002).